# Habitual Physical Activity Preserves Energetically Constrained Mitochondrial Programs During Human Skeletal Muscle Aging

Ceereena Ubaida-Mohien, Stefano Donega, Alexey Lyashkov, Yevgeniya Lukyanenko, Shepherd H. Schurman, Arsun Bektas, Jaekwan Kim, Perry Kuo, Linda Zukley, Mary Kaileh, Kenneth Fishbein, Nan-Ping Weng, Chee W. Chia, Ranjan Sen, María Carmen Gómez-Cabrera, Luigi Ferrucci

## Supplementary Tables

### Supplementary Table S1. Definitions of key variables and derived metrics used in this study

| **Term** | **Definition** | **Type** | **Notes** |
|---|---|---|---|
| **Age** | Chronological age in years (23 to 86 years, n=96) | Clinical variable | Modeled as continuous variable |
| **Habitual Physical Activity** | Self-reported physical activity level (0-3: Not active to Highly active) | Behavioral exposure | Treated as ordinal numeric variable in regression models |
| **$VO_2$peak** | Peak oxygen consumption ($mL \cdot kg^{-1} \cdot min^{-1}$) | Physiological exposure | Measure of cardiorespiratory fitness.<br>Used for rescue classification and energetic alignment score |
| **kPCr** | Phosphocreatine recovery rate constant ($s^{-1}$) | Physiological outcome | Proxy for mitochondrial ATP production capacity |
| **Mito$O_2$Flux (respirometry)** | Skeletal muscle mitochondrial oxygen consumption rate | Physiological energetic measure | Used in correlation analyses with mitochondrial proteome scores (Fig. 4A) to validate energetic coupling |
| **MitoCoP** | Curated database of high-confidence mitochondrial proteins (n = 1,134) | Annotation resource | Used to define mitochondrial protein set |
| **Mitochondrial Proteome (Mito proteins)** | Proteins annotated as mitochondrial by MitoCoP (n = 741 in dataset) | Protein subset | Background for pathway enrichment |

| | | | |
|---|---|---|---|
| **Age-associated proteins** | Proteins with p-value_age < 0.05 in age regression model | Derived set | Significance based on linear regression |
| **PA-associated proteins** | Proteins with p-value PA < 0.05 in PA model | Derived set | Direction interpreted relative to age |
| **$VO_2$**peak**-associated proteins** | Proteins with p-value $VO_2$peak < 0.05 in $VO_2$peak model | Derived set | Used for rescue comparison |
| **Rescued proteins** | Proteins with significant age ($p<0.05$) and exposure effects in opposing directions | Derived classification | $\beta$_age < 0 & $\beta$_exposure > 0 OR $\beta$_age > 0 & $\beta$_exposure < 0 |
| **Rescue (Normalized proteins)** | Proteins with age↑ and exposure↓ pattern | Derived classification | Used in rescue direction analysis |
| **Non-rescued proteins** | Proteins not meeting directional rescue criteria | Derived classification | Includes concordant directional effects or nonsignificant exposure effects |
| **MitoScore (741)** | Mean standardized abundance across all quantified MitoCop annotated mitochondrial proteins (n=741) | Composite score | Full quantified mitochondrial abundance metric |
| **OxPhosScore (116)** | Mean standardized abundance of all oxidative phosphorylation proteins (n=116) | Composite score | OxPhos-focused metric |
| **AgeMitoScore** | Mean standardized abundance of age-associated mitochondrial proteins (n=195) | Composite score | Reflects degree of age-associated remodeling |
| **PA-MitoScore** | Mean standardized abundance of PA-associated mitochondrial proteins (n=231) | Composite score | Reflects degree of PA-associated remodeling |
| **PA-Rescued Score** | Mean standardized abundance of physical activity-rescued mitochondrial proteins (n= 76, PA p-value < 0.05) and age p-value < 0.05) | Composite score | Molecular signature of physical activity-aligned rescue |
| **$VO_2$**peak **Rescued Score** | Mean standardized abundance of $VO_2$peak- | Composite score | Molecular signature of fitness-aligned rescue |

| | | | |
|---|---|---|---|
| | rescued mitochondrial proteins (n=163) | | |
| **Physical activity-Rescue Tertiles** | Low / Medium / High groups defined by tertiles of PA-RescuedScore | Stratification variable | Used in energetic and network analyses |
| **Composite systemic mitochondrial score** | Mean of tissue-specific standardized mitochondrial scores (z-scores) across PBMCs, naïve CD4 T cells, naïve CD8 T cells, and skin for each individual | Composite score | Higher values indicate greater multi-tissue mitochondrial abundance. |
| **Systemic Mitochondrial Coordination** | Correlation structure among mitochondrial scores across tissues | Network metric | Assessed using Spearman correlations |
| **Network Density** | Proportion of tissue–tissue correlations exceeding threshold | Graph metric | Calculated as the number of tissue-tissue correlation pairs with |

**Supplementary Table S2. Definitions of mitochondrial proteomic scores and summary statistics for energetic coupling analyses**

| **Section** | **Item** | **Definition / model** | **N / protein set size** | **Key result** |
|---|---|---|---|---|
| **a. Panel-specific statistics** | **Fig. 4a** | Raw correlation: Age vs $VO_2$peak | 96 participants | r = −0.69 |
| | | Raw correlation: Age vs kPCr | 96 participants | r = −0.36 |
| | | Raw correlation: $VO_2$peak *vs* kPCr | 96 participants | r = 0.48 |
| | | Raw correlation: PA-rescued score vs kPCr | 96 participants | r = 0.34 |
| | | Raw correlation: PA-rescued score vs $VO_2$peak | 96 participants | r = 0.15 |
| | | Partial correlation: PA-rescued score vs kPCr, adjusted for age | complete cases | partial r = 0.43, $P = 9.96 \times 10^{-5}$ |

| | | | | |
|---|---|---|---|---|
| **b. Panel-specific statistics** | **Fig. 4b** | Mixed-effects model: RescueScore ~ AgeMitoScore * RescueType + kPCr_group + (1 \| DonorID) | 96 donors; 192 observations | AgeMitoScore $\beta$ = 1.361; AgeMitoScore × VO$_2$peak-rescued $\beta$ = −0.271; kPCr-high $\beta$ = 0.0109 |
| | **Fig. 4c** | kPCr compared across tertiles of PA-rescued score | 96 participants | Kruskal–Wallis P = 0.002 |
| | **Fig. 4d (complete-case)** | physio_energy ~ age_c + pa_score_z | 78 participants | age: $\beta = -0.023$, $P = 8.3 \times 10^{-9}$; PA score: $\beta = 0.36$, $P = 1.7 \times 10^{-6}$; $R^2 = 0.54$ |
| | **Fig. 4d (interaction test)** | physio_energy ~ age_c * pa_score_z | 78 participants | age × PA score: $\beta = -0.0046$, $P = 0.18$ |
| | **Fig. 4d (multiple imputation)** | Pooled linear model after predictive mean matching imputation of kPCr and VO$_2$peak | imputed dataset | age: $\beta = -0.0208$, 95% CI −0.0284 to −0.0133, $P = 9.6 \times 10^{-7}$; PA score: $\beta = 0.315$, 95% CI 0.168 to 0.462, $P = 6.8 \times 10^{-5}$ |
| **C. Protein-level overlap / enrichment** | **Fig. 4e** | Mitochondrial proteins associated with kPCr after adjustment for age and covariates | 741 proteins tested | 366 proteins associated with kPCr |
| | | PA-rescued proteins also associated with kPCr | 76 PA-rescued proteins | 71/76 (93%) nominally associated with kPCr ($P < 0.05$) |
| | | Enrichment of PA-rescued proteins among kPCr-associated mitochondrial proteins | mitochondrial functional category level | odds ratio = 17.6, 95% CI 7.1–56.5, $P < 2.2 \times 10^{-16}$ |

Footnote: All proteomic scores were calculated as the mean standardized abundance (z-score) of member proteins per participant. Rescue classes were defined by opposite signs of exposure-associated and age-associated regression coefficients. age_c denotes age centered at 60 years.

# Supplementary Figures

## Supplementary Fig. 1. Aging selectively drives remodeling of the skeletal muscle mitochondrial proteome

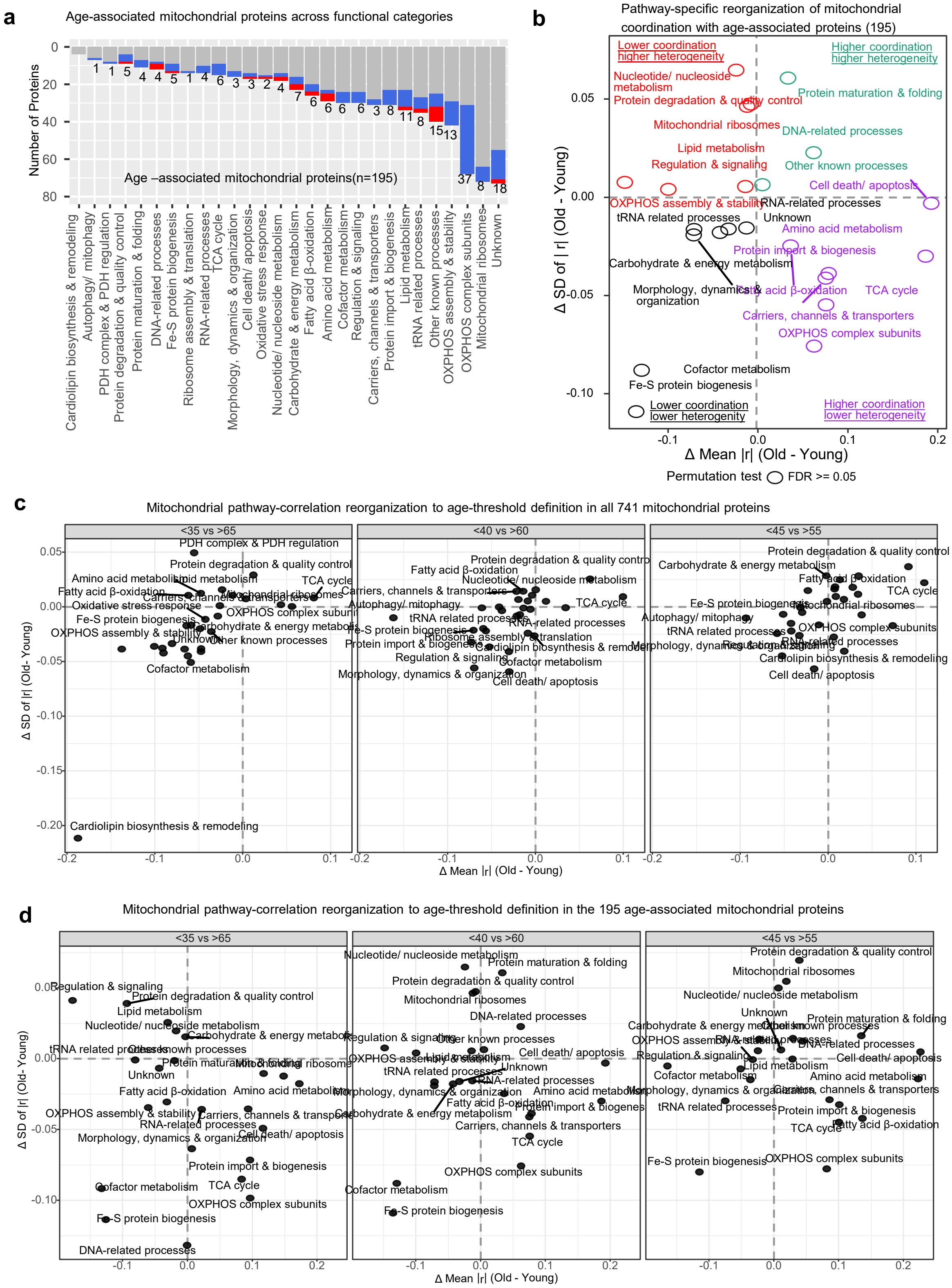

**Supplementary Fig. 1. Aging selectively drives remodeling of the skeletal muscle mitochondrial proteome. a,** Age-associated mitochondrial proteins across functional categories. Bar plot shows the number of quantified mitochondrial proteins within each functional category. The number of proteins showing significant age-associated increases or decreases in abundance is indicated adjacent to each bar. **b,** Pathway-level mitochondrial correlation reorganization in the 195 age-associated mitochondrial subset. **c,** Sensitivity of mitochondrial pathway-correlation reorganization to age-threshold definition in all 741 mitochondrial proteins. Pathway-level changes in correlation strength and heterogeneity were recalculated using alternative young/old thresholds. Pathway-level changes in within-category correlation strength (Δ mean |r|) and correlation heterogeneity (Δ SD of |r|) were recalculated using alternative age-group definitions (<35 vs >65, <40 vs >60, and <45 vs >55). **d,** Sensitivity of mitochondrial pathway-correlation reorganization to age-threshold definition in the 195 age-associated mitochondrial proteins. The age-sensitive subset showed broadly similar pathway-level patterns across threshold definitions, with greater stability for changes in mean within-pathway correlation than for changes in correlation heterogeneity. The overall pattern was more pronounced in the age-associated subset, and pathway-level changes in mean correlation were more stable across threshold definitions than changes in correlation heterogeneity.

**Supplementary Fig 2. Habitual physical activity preserves bioenergetic components of the aging mitochondrial proteome**

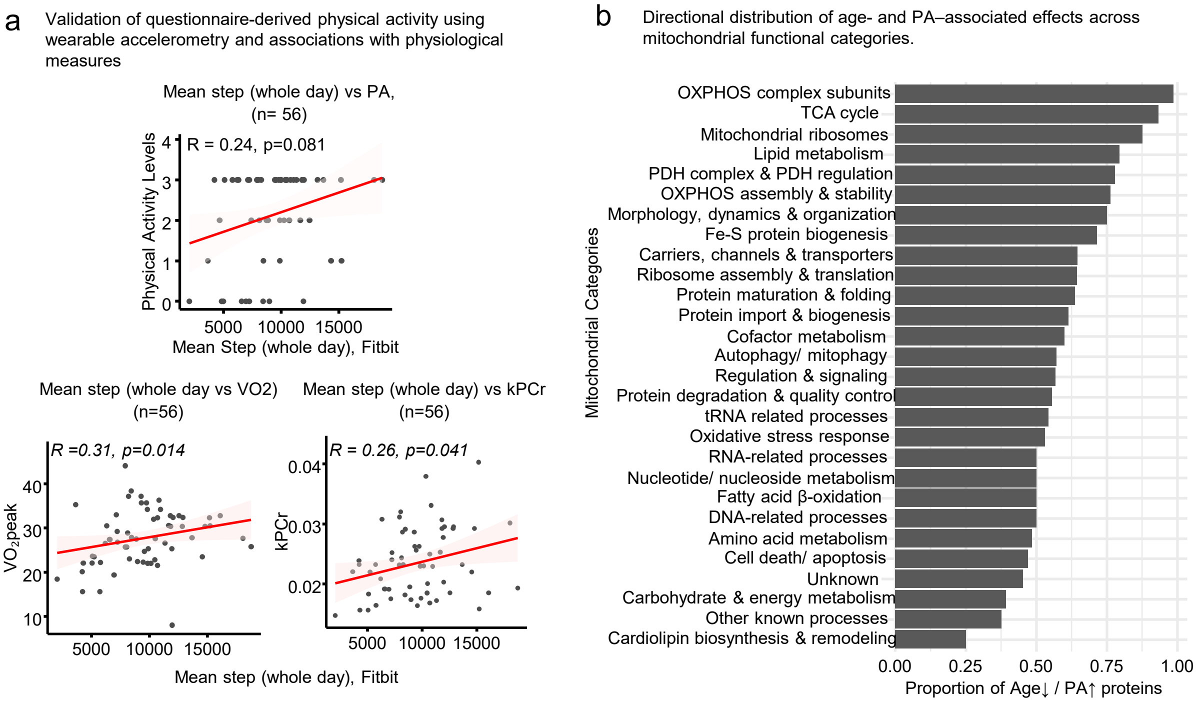
a Validation of questionnaire-derived physical activity using wearable accelerometry and associations with physiological measures

b Directional distribution of age- and PA–associated effects across mitochondrial functional categories.

**Supplementary Fig. 2. Habitual physical activity preserves bioenergetic components of the aging mitochondrial proteome. a,** Validation of questionnaire-derived physical activity using wearable accelerometry and associations with physiological measures. (Top) Association between questionnaire-derived physical activity (four-level ordinal variable, 0–3) and mean daily step count measured by wearable accelerometry in a subset of participants (n = 56). (Bottom)

Relationship between mean daily step count and $VO_2$peak. Relationship between mean daily step count and kPCr. Lines represent linear regression fits with 95% confidence intervals. Statistical significance was determined using Spearman correlation. **b,** Proportion of annotated mitochondrial proteins (n = 741) within each functional category exhibiting concordant directional associations with age and physical activity. Bars show the percentage of proteins displaying age-associated decreases with activity-associated increases (Age↓/PA↑) or age-associated increases with activity-associated decreases (Age↑/PA↓). Across mitochondrial categories, the proportion of proteins shows the Age↓/PA↑ pattern ranged from ~34% to 99%.

**Supplementary Fig 3. Cardiorespiratory fitness strongly opposes age-related remodeling of the mitochondrial proteome**

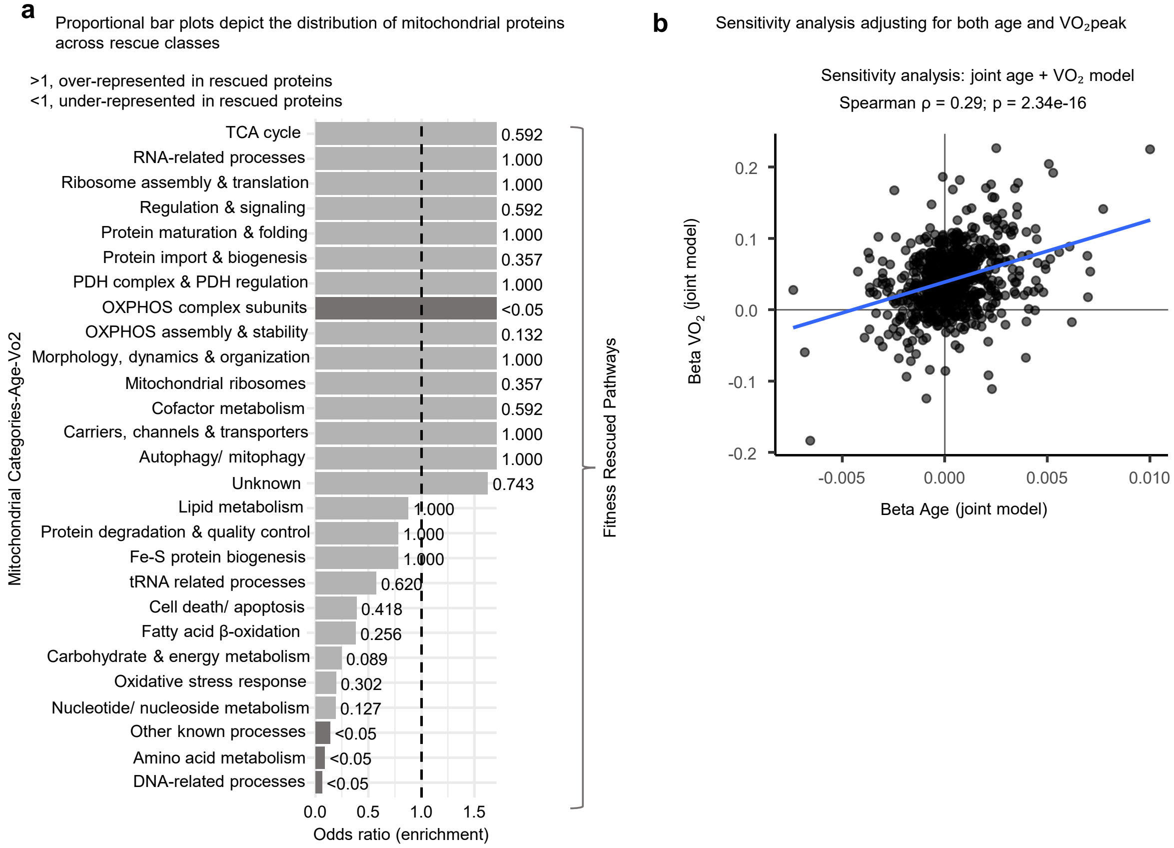

**Supplementary Fig. 3. Cardiorespiratory fitness strongly opposes age-related remodeling of the mitochondrial proteome**. **a,** Odds ratios show enrichment or depletion of $VO_2$-rescued proteins across mitochondrial functional categories relative to the remainder of the annotated mitochondrial proteome. Categories with odds ratios greater than 1 are enriched for $VO_2$-rescued proteins, whereas categories with odds ratios less than 1 are depleted. **b,** Sensitivity analysis adjusting for both age and $VO_2$peak. Scatterplot showing the relationship between regression coefficients for age and $VO_2$peak derived from linear models including both predictors simultaneously (protein ~ age + $VO_2$peak + covariates). Each point represents a mitochondrial protein. Spearman correlation coefficient ($\rho = 0.29$, $P = 3.1 \times 10^{-16}$) is shown.

## Supplementary Fig 4. Mitochondrial proteomic signatures are coupled to energetic capacity across molecular and physiological levels

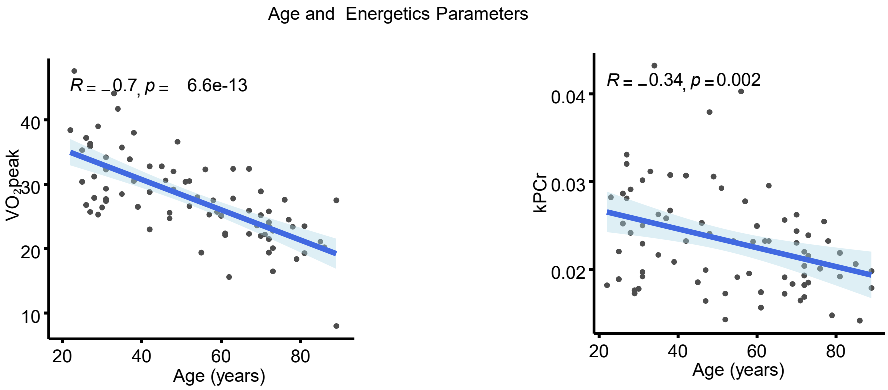

**Supplementary Fig 4. Associations of age with $VO_2$peak and kPCr in 96 GESTALT participants**. Left, age and $VO_2$peak. Right, age and kPCr. Each gray circle represents one participant. Associations between age. kPCr and $VO_2$peak were assessed using two-sided Pearson correlation, the blue line shows the least-squares linear regression fit with 95% confidence interval.

## Supplementary Fig 5. PA-rescued muscle mitochondrial signatures are associated with altered cross-tissue mitochondrial coordination

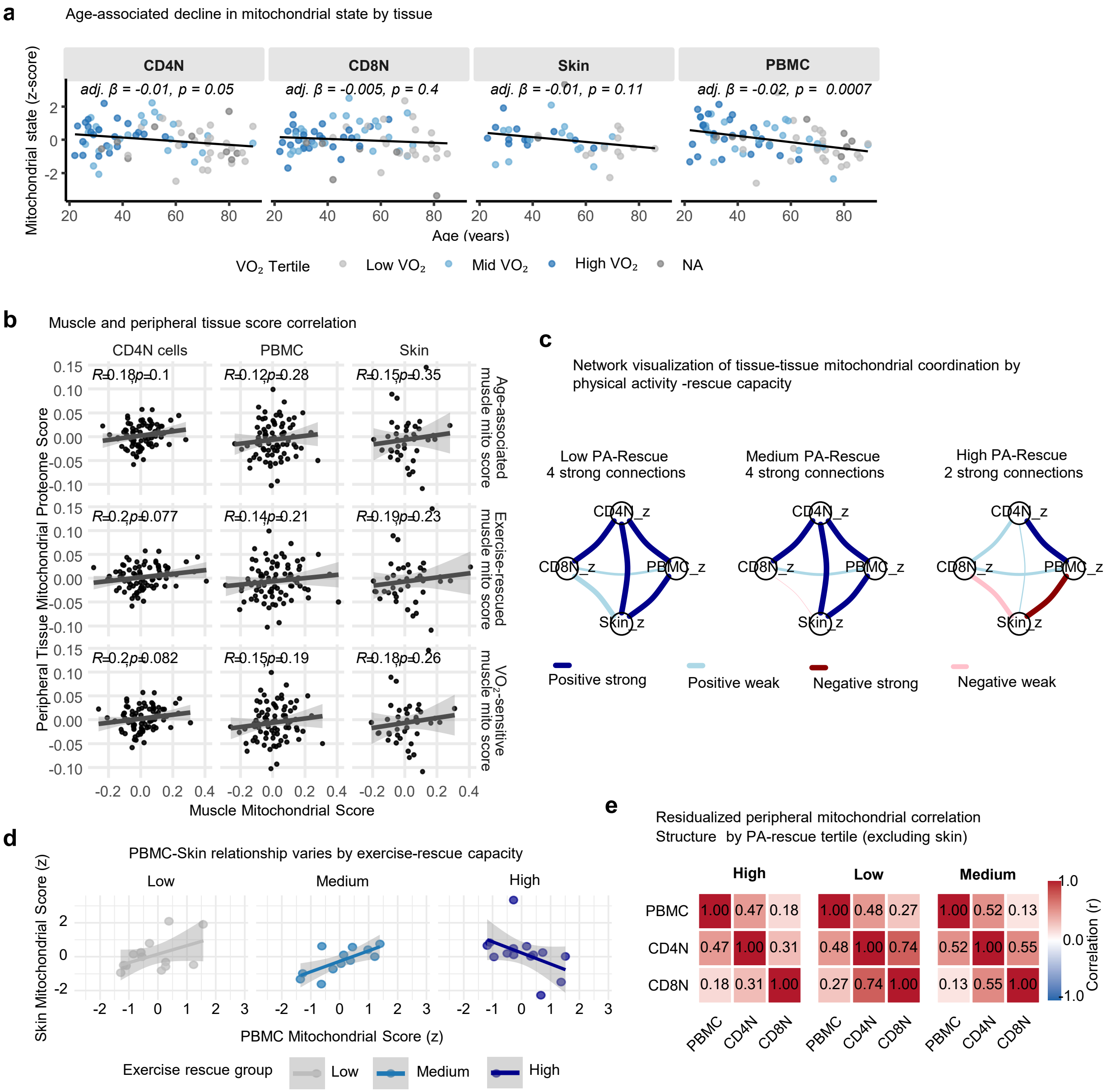

| | High PBMC | High CD4N | High CD8N | Low PBMC | Low CD4N | Low CD8N | Medium PBMC | Medium CD4N | Medium CD8N |
|---|---|---|---|---|---|---|---|---|---|
| PBMC | 1.00 | 0.47 | 0.18 | 1.00 | 0.48 | 0.27 | 1.00 | 0.52 | 0.13 |
| CD4N | 0.47 | 1.00 | 0.31 | 0.48 | 1.00 | 0.74 | 0.52 | 1.00 | 0.55 |
| CD8N | 0.18 | 0.31 | 1.00 | 0.27 | 0.74 | 1.00 | 0.13 | 0.55 | 1.00 |

**Supplementary Fig.5 PA-rescued muscle mitochondrial signatures are associated with altered cross-tissue mitochondrial coordination**. **a,** Heterogeneous association of age with mitochondrial score across systemic tissues. Scatterplots showing the association between participant age (x-axis) and the normalized mitochondrial state z-score (y-axis) across four systemic tissues. Each point represents an individual participant, colored according to their $VO_2$max tertile (Low, gray; Mid, light blue; High, dark blue). The solid black line in each panel represents the unadjusted linear regression fit for visual guidance. Beta coefficient (adj. β) and corresponding p-value (adj. p) for the age term, derived from a multiple linear regression model adjusting for participant sex and BMI. **b,** Muscle and peripheral tissue score correlation. Each point represents an individual participant. **c**, Network representation of peripheral mitochondrial correlation structure by PA-rescue tertile. Nodes represent PBMCs, CD4N, CD8N cells, and skin, and edges represent pairwise correlations based on mitochondrial scores. Edge width reflects absolute correlation magnitude and edge color indicates sign. **d,** PBMC-Skin mitochondrial score reverses directionality with physical activity -rescue tertile. Scatter plots show the relationship between PBMC mitochondrial score (x-axis, z-score) and skin mitochondrial score (y-axis, z-score) stratified by physical activity -rescue capacity tertiles. Gray = low rescue ($r = 0.2$, $p = 0.51$), light blue = medium rescue ($r = 0.74$, $p < 0.009$), dark blue = high rescue ($r = -0.31$, $p < 0.26$). Lines represent linear regression with 95% confidence intervals (shaded regions). $n = 32$ per group. **e,** Residualized peripheral mitochondrial correlation structure excluding skin. Heatmaps show pairwise correlations among residualized mitochondrial scores from PBMCs, CD4N, and CD8N T cells within low, medium, and high PA-rescue tertiles. Tissue scores were residualized for age, sex, BMI, and fiber ratio before within-group correlation analysis. Compared with the full peripheral analysis including skin, group differences were attenuated, indicating that the principal cross-compartment shifts were driven primarily by skin-linked relationships. A weaker residual pattern remained among blood-derived compartments, particularly reduced CD4N and CD8N T-cell correlation in the high PA-rescue group.